Tuning Magnetism of Metal Porphyrazine Molecules by Ferroelectric In_2Se_3 Monolayer

Xiao Tang[1], Jing Shang[1], Yandong Ma[2], Yuantong Gu[1], Changfeng Chen[3*], and Liangzhi Kou[1*]

[1] School of Mechanical, Medical and Process Engineering, Queensland University of Technology, Brisbane, QLD 4001, Australia

[2] School of Physics, State Key Laboratory of Crystal Materials, Shandong University, Jinan 250100, China

[3] Department of Physics and Astronomy, University of Nevada, Las Vegas, Nevada 89154, United States

*chen@physics.unlv.edu

* liangzhi.kou@qut.edu.au

Abstract: Electric tuning of magnetism is highly desirable for nanoelectronics, but volatility in electron spin manipulation presents a major challenge that needs urgent resolution. Here we show by first-principles calculations that magnetism of metal porphyrazine (MPz) molecules can be effectively tuned by switching ferroelectric polarization of an adjacent In_2Se_3 monolayer. The magnetic moments of TiPz and VPz (MnPz, FePz, and CoPz) decrease (increase) at one polarization but remain unchanged at reversed polarization. This intriguing phenomenon stems from distinct metal *d*-orbital occupations caused by electron transfer and energy-level shift associated with the polarization switch of In_2Se_3 monolayer. Moreover, ferroelectric switch also tunes underlying electronic properties, producing metallic, half-metallic or semiconducting state depending on polarization. These findings of robust ferroelectric tuning of magnetism and related electronic properties in MPz adsorbed In_2Se_3 hold great promise for innovative design and implementation in advanced magnetic memory storage, sensor and spintronic devices.

Keywords: ferroelectric controlled magnetism, metal porphyrazine molecules, ferroelectric switch of In_2Se_3, *d* orbital shift, first-principles calculations

1. Introduction

Tuning magnetism by electric field is a long-sought goal in materials research with great potential for applications.[1-4] Manipulation of electronic spin via electric field provides an effective way to modulate key quantum states in nanosized structures and devices.[5-7] Since early reports on dilute magnetic semiconductors like (In,Mn)As,[8] materials exhibiting magnetic response to electric tuning have attracted great interest. Their working principles mainly fall into three categories. In magnetic semiconductors, electric field alters carrier concentration to mediate magnetic interaction.[9-11] In magnetic metals, electric field shifts the Fermi energy to influence interface magnetic anisotropy.[12-14] In multiferroics, magnetoelectric coupling tunes magnetic behaviors via electric polarization. In ferromagnetic-ferroelectric heterostructures, for instance, an external electric field induces lattice changes in ferroelectric crystals, which in turn influence adjacent ferromagnetic layers, thereby manipulating the magnetic behavior.[15-19]

Recent years have seen significant progress in research on electric tuning of magnetism, but some major issues remain to be resolved.[8, 20] Manipulating magnetism in a well-controlled manner is among the most challenging. For example, while dielectric gating is effective in manipulating magnetic properties, large electric fields required to achieve such a feat may damage the structure.[21] Another issue for the electric tuning of magnetism concerns persistent electric power to retain the magnetic state, leading to considerable energy waste. Promising solutions to these problems are offered by recently emerging ferroelectric materials that possess two polarized states (P ↑ and P ↓) energetically degenerate and quickly switchable by external stimuli to enable nonvolatile information storage. When external electric field is retracted, the polarization remains stable, thus avoiding the need for continuous power supply. Consequently, ferroelectrics are promising materials for effective modulation and control of the properties of other materials. For instance, ferroelectric switching of Sc_2CO_2 was used to control electronic properties of CrI_3 monolayer and achieve transitions between semiconducting and half-metallic states.[22] Meanwhile, the interlayer magnetic coupling of CrI_3 bilayer also can be controlled by polarization reversal.[23] Stacking ferromagnetic and ferroelectric layers, the magneto-crystalline anisotropy of the ferromagnetic layer can be changed, providing new platforms for magnetic memory.[24] In all these cases, however, energy differences between different magnetic states are very small, and thermal fluctuations may make it hard to stabilize the desired phenomena.

In this work, we present a compelling case of effective tuning of magnetic moment by ferroelectric switch. We chose α-In_2Se_3 monolayer as the ferroelectric material due to its robust out-of-plane ferroelectricity that has been experimentally observed at room temperature.[25, 26] Metal porphyrazine (MPz) molecules with intrinsic magnetism are chosen as the objects to be modulated by the ferroelectric switch. MPz are well known for their catalytic properties,[27-29] multiferroic MPz molecules find applications in nonvolatile memory devices.[30] Using density-functional theory calculations, we show that magnetic behaviors of MPz molecules can be well tuned by the polarization of ferroelectric In_2Se_3 layer. In contrast to the weak magnetic coupling or small magneto-crystalline anisotropy energy in previous reports, here the magnetic moment is significantly modulated by the ferroelectric switch.[23-24] For instance, the magnetism of TiPz can be switched OFF/ON when the polarization direction of In_2Se_3 monolayer is reversed, acting as an effective magnetic switch. Moreover, it is also found that the system can host metallic, half-metallic and semiconducting states depending on the ferroelectric polarization direction. These findings of ferroelectric controlled magnetic and electronic properties in MPz-In_2Se_3 structure raise exciting prospects for innovative device applications.

2. Methods

Results reported in this work were obtained from calculations based on the spin-polarized density-functional theory (DFT) as implemented in the Vienna ab initio Simulation Package (VASP) and with the adaptation of the projector augmented wave method.[31-33] The generalized gradient approximation (GGA) in the form of Perdew-Burke-Ernzerhof (PBE) was adopted for the exchange and correlation functional.[34] To properly describe partially filled metal d-orbitals, the GGA+U method[35] with U = 4 eV and J = 1 eV was adopted. These values of the interaction parameters were chosen based on tests results obtained in previously reported works.[36, 37] We have further tested different values for U (U=3, 3.5 eV) and obtained similar results on the main material properties shown in the present work. To model the In_2Se_3 monolayer structure, a $2\sqrt{3} \times 2\sqrt{3}$ supercell was used with a vacuum layer larger than 15 Å to avoid self-interaction. A cut-off energy of 400 eV and a Γ-centered 3×3×1 Monkhorst-Pack k mesh were chosen. All the atomic structures were relaxed until the forces on all the atoms were less than 0.01 eV/Å and the convergence criteria for energy was set to 1×10^{-5} eV. The van der Waals (vdW) interaction

between MPz molecules and In_2Se_3 monolayer was described by the DFT-D3 method.[38] The adsorption energy (E_{ads}) between MPz molecules and In_2Se_3 monolayer is determined by

$$E_{ads} = E_{total} - E_{MPz} - E_{In2Se3}$$

where E_{total}, E_{MPz} and E_{In2Se3} are energies of the MPz adsorbed In_2Se_3 monolayer, isolated MPz molecules, and freestanding In_2Se_3 monolayer, respectively.

3. Results

3.1 Ferroelectric dependent adsorption energy and electron transfer

Metal complexes of N_4-ligands (Figure 1a) have been synthesized and widely used for chemical photocatalysis[39, 40]; In_2Se_3 monolayer has been synthesized with out-of-plane ferroelectricity theoretically predicted and experimentally confirmed.[25, 26, 41]. The In_2Se_3 monolayer comprises a quintuple atomic layer structure connected in the sequence of Se-In-Se-In-Se (Figure 1b); its polarization can be reversed by shifting the position of the middle Se layer[40]. Calculated lattice constants, layer height, and interlayer distances (Table S1) are all consistent with experimental data.[41-44] The asymmetric substrate leads to two different structural models for MPz (M=Sc-Zn) adsorption on In_2Se_3 monolayer, depending on the polarization direction (Figure 1c and 1d).

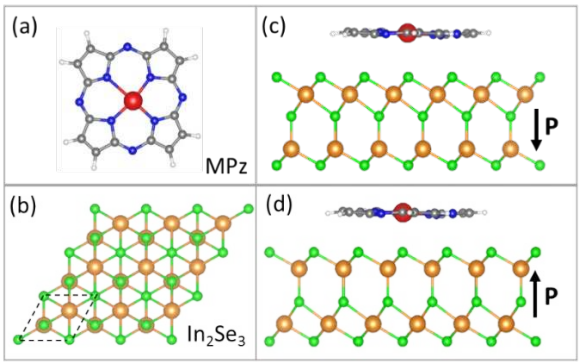

Figure 1. Top views of (a) MPz and (b) In_2Se_3. The unit cell of In_2Se_3 is denoted by black dashed lines. The white, blue, grey, red, green, orange spheres represent H, N, C, transition metal, Se and In atoms, respectively. Side views of MPz adsorbed In_2Se_3 monolayer in (c) P ↓ and (d) P ↑ polarized states.

For freestanding MPz molecules (M = Sc, Ti and V), their relatively large ionic radii make the molecular structure buckled, producing an out-of-plane polarization.[30] When such molecules are

placed on In_2Se_3 monolayer, their intrinsic polarization couples with the ferroelectric polarization of the In_2Se_3 substrate, leading to different adsorption energy and electron transfer depending on the relative directions of the polarization. Consequently, these MPz molecules (M = Sc, Ti and V) prefer to adsorb on the In_2Se_3 surface with P↓ polarization, as reflected by the larger absolute value of adsorption energies shown in Figure 2a. Taking ScPz molecule as an example, due to the different scenarios of polarization superposition and cancellation (Figure S1), the adsorption energy on the P↓ surface is -2.82 eV, which is considerably higher than -2.12 eV on the opposite surface. For MPz molecules with M=Cr, Mn, Fe, the absolute values of adsorption energy on the P↓ surface are also larger, although there is no obvious structural buckling and no out-of-plane polarization, indicating that additional mechanisms other than the molecular buckling induced polarization are also responsible for the preferred surface adsorption, which will be discussed below. For the adsorption energy of the remaining MPz (M=Ni, Cu and Zn) molecules, no obvious surface dependence is found, which likely stems from the large equilibrium distances up to 3.4 Å between Ni, Cu, Zn-Pz molecules and In_2Se_3 monolayer, placing it in the range of weak van der Waals interaction (see Figure S2).

The dependence of adsorption energy on ferroelectric polarization is ascribed to the electrostatic potential difference ($\Delta\Phi$) between the MPz molecule and In_2Se_3 monolayer and the associated electron transfer. The breaking of the centrosymmetric In_2Se_3 structure by MPz adsorption leads to an out-of-plane spontaneous electric polarization, resulting in $\Delta\Phi$=1.20 eV (calculated at the PBE level) between the top and bottom surfaces (Figure 2d), in accordance with previously studies.[41, 42] When MPz molecules are adsorbed on the P↓ surface, the value of $\Delta\Phi$ is much larger than that on the P↑ surface. For TiPz molecule, $\Delta\Phi$ is 0.45 eV on the P↑ surface, but reaches 1.65 eV when the polarization is switched to P↓. More electrons are transferred between MPz and In_2Se_3 when the molecule is on the P↓ surface, as seen in Figure 2b and 2c. The adsorption energy is also larger for other MPz-In_2Se_3 (P↓) systems, but for M=Ni, Cu, Zn, there is little electron transfer in both polarizations, leading to insensitive adsorption energies.

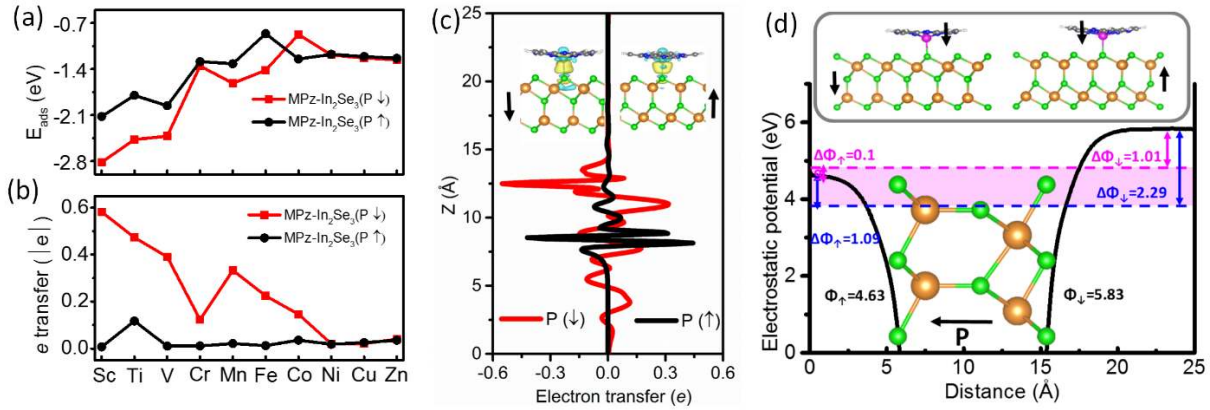

Figure 2. (a) Adsorption energy and (b) electron transfer of MPz-In_2Se_3 with P↑ or P↓ polarization. (c) Electron transfer of VPz on In_2Se_3. The charge differences induced by the VPz adsorption are shown in the inset, where the cyan (yellow) shade indicates electron loss (accumulation), and the isosurface value is set to 0.002 e $Å^{-3}$. (d) Electrostatic potentials of In_2Se_3 (black line) and all MPz molecules (pink region). Blue and pink dashed lines denote, respectively, the lowest and highest electrostatic potential among all the MPz (M=Sc-Zn) molecules. Insets show the structural configurations of TiPz molecule adsorbed on In_2Se_3 monolayer.

3.2 Ferroelectric tuning of magnetism

Most freestanding MPz molecules studied in this work are magnetic, except for those with M being Sc, Ni, or Zn. The behaviors of these magnetic MPz molecules can be understood based on the '4+1' splitting rule for a transition metal atom surrounded by the porphyrin ligand, which usually results in four orbitals close in energy and one high-lying orbital.[45, 46] Taking TiPz molecule as an example, the metal Ti ($3d^2 4s^2$) electrons form bonding states with the porphyrin ligand, leaving two electrons in the *d* orbitals unoccupied, therefore producing the magnetic moment of about 2 μ_B (values are not exactly 2 μ_B due to the effect of on-site U repulsion). For VPz ($3d^3 4s^2$) and CrPz ($3d^4 4s^2$), the additional electrons occupy the majority spin state, thus enhancing the magnetic moment to around 3.0 and 4.0 μ_B per unit cell, respectively. Further increasing electrons in the d orbitals of MnPz ($3d^5 4s^2$), FePz ($3d^6 4s^2$) and CoPz ($3d^7 4s^2$) occupy the minority spin states and reduce the magnetic moment to about 3, 2 and 1 μ_B, respectively. For NiPz ($3d^8 4s^2$), all four d orbitals for both spins are occupied, leading to zero moment.

When a MPz molecule is placed on In_2Se_3 monolayer in the P↑ state, its magnetic moment remains almost unchanged (black line in Figure 3a). In contrast, an obvious change in magnetic moment occurs when the molecule is on the P↓ surface (red line in Figure 3a). It is interesting to note that the magnetic moments of TiPz and VPz are reduced while the values for MnPz, FePz

and CoPz are increased, indicating that magnetism can be controlled by the ferroelectric switch of In_2Se_3. The magnetic moment of TiPz is 1.25 μ_B when it is on the P ↑ surface, but 0 μ_B on the P ↓ surface, indicating that magnetism of Ti-MPz can be switched ON/OFF when the polarization direction of In_2Se_3 monolayer is reversed. Meanwhile, for FePz molecule, the magnetic moment is 2.0 μ_B on the P ↑ surface and 2.3 μ_B on the P ↓ surface. The ferroelectric controlled magnetism can be understood based on the rule of '4+1' *d* orbital splitting and electron transfer illustrated in Figure 2b. From Figure 3c and 3d, it is seen that MPz molecules on the P ↓ surface have remarkable electron transfer, causing changes in electron configurations of 3*d* orbitals in MPz molecules and the corresponding magnetic moment; in contrast, electron transfer is trivial when the molecule is on the P ↑ surface leaving the magnetic moment almost unchanged. For example, the magnetic moment of VPz decreases from 2.94 μ_B on In_2Se_3 (P ↑) to 2.23 μ_B on In_2Se_3 (P ↓). The electronic configuration of V^{2+} is [Ar] $3d^3$ with three unpaired *d* electrons giving rise to about 3 μ_B magnetic moment in free VPz as analyzed above. This magnetic configuration is preserved in VPz-In_2Se_3 (P ↑) since electron transfer in this configuration is trivial as shown in Figure 2c, with the occupation of *d* orbitals barely changed. In contrast, when this molecule is on In_2Se_3 (P↓), a large amount of electron (~0.39 e as evaluated from Bader charge analysis[47]) is transferred from VPz to In_2Se_3 (P ↓), with one majority spin electron state partially occupied (Figure 3c) and the magnetic moment decreased to 2.23 μ_B. For MnPz, the magnetic moment increases from 3.09 μ_B (P ↑) to 3.53 μ_B (P ↓) under the ferroelectric switch of the substrate. The electronic configuration of Mn^{2+} is [Ar] $3d^5$, with four *d* electrons occupying the majority spin states while one electron occupying the minority spin state based on the '4+1' rule, giving rise to a magnetic moment of about 3 μ_B. The significant electron transfer from MPz molecule to the substrate (0.36 e) reduces the occupation of the minority spin state, leading to the increase of the overall magnetic moment (3.53 μ_B) under the P ↓ state, see Figure 3d. We further checked the magnetic variation of VPz by artificially changing the interlayer distance from the substrate. As shown in Figure S3, the magnetic moment of VPz-In_2Se_3 (P ↓) increases to the value of the freestanding molecule when the interlayer distance is enlarged, while that of VPz-In_2Se_3 (P↑) remains almost unchanged due to the trivial electron transfer at the equilibrium position. It is worth noting that the magnetic moment of VPz-In_2Se_3 (P↓) is still smaller than that of VPz-In_2Se_3 (P↑) when the interlayer distance is up to 5

angstroms, where the electron transfer is trivial. This result implies that beside electron transfer, the *d*-orbital shift by polarization is also responsible for the ferroelectric tuning of magnetism. For ScPz, it is always non-magnetic regardless of the polarization direction of In_2Se_3, due to the empty *d* orbital from the electronic configuration of Sc^{3+} [Ar] $3d^0$. However, the band states near the Fermi level are affected by the polarization, leading to different hybridizations with the substrate (Figure S4) and polarization dependent electron transfers, see Figure 2. Since the polarization direction of ferroelectric materials is switchable by an external bias, based on the successful control of ferroelectric domains in experiment, the magnetic moment of MPz is expected to be controllable when the bias is reversed.

For a comparative study, we present the projected density of states (PDOS) of V in the VPz-In_2Se_3 (Figure 3b) and in VPz molecule. For the freestanding VPz molecule, only the majority spin states d_{z^2}, d_{xz} and d_{yz} are occupied (see inset in Figure 3c), leading to the magnetic moment of about 3 μ_B, which is consistent with above analysis based on the '4+1' rule of the *d*-orbital splitting. Upon exposure to In_2Se_3 (P ↑), although the d_{z^2} orbital is lifted to the conduction band area, the d_{xy} orbital is occupied by the majority spin state, therefore keeping the magnetic moment unchanged. When VPz is placed on top of In_2Se_3 (P ↓), d_{xz} orbital is lifted by the polarization to the Fermi level, becoming half occupied (see the state crossing the Fermi level indicated in Figure 3b), hence reducing the magnetic moment to 2.23 μ_B. For other MPz molecules interacting with the In_2Se_3 P ↓ or P ↑ state, similar behaviors of the *d*-orbital shifting are observed, see Supporting Materials (Figure S5-6). Since the MPz molecules are weakly absorbed on the In_2Se_3 surface with van der Waals interactions, the adsorption configurations may be different from the most stable ones shown in Figure 1. To check the effects of adsorption configurations on the energetic and magnetic properties, we also have calculated these values when MPz molecules have a shift and rotation relative to the most stable structure, see Figure S7. It is found that the polarization dependent adsorption energy and magnetic moment at different configurations remain essentially unchanged, indicating the robustness of our findings.

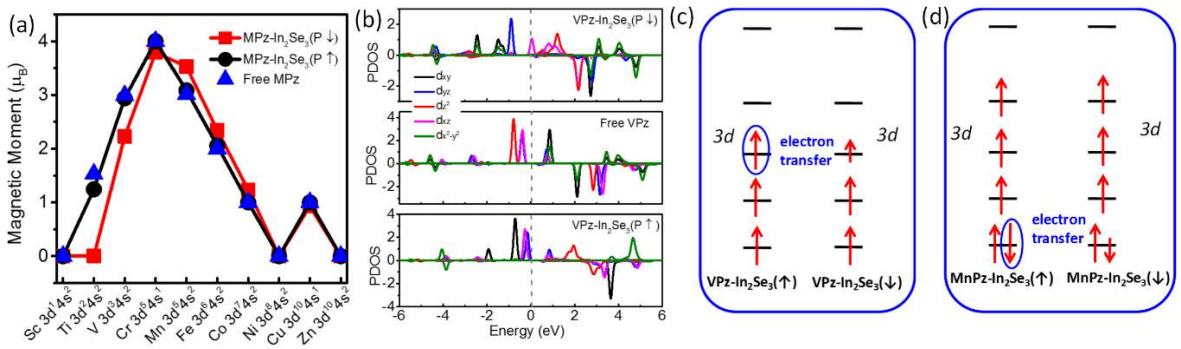

Figure 3 (a) Total magnetic moment of MPz-In_2Se_3 (P ↑ or P ↓). (b) PDOS of V in the VPz adsorption system and in a freestanding VPz molecule. The Fermi level is set to zero. Schematic representations of the electronic structures of (c) VPz-In_2Se_3 (P ↑ or P ↓) and (d) MnPz-In_2Se_3 (P ↑ or P ↓).

3.3 Ferroelectric tuning of electronic properties and electric-field effects

Ferroelectric switch also has major impacts on electronic properties via electron doping effects and orbital shifting induced by the change of polarization, causing the electronic states near the Fermi level to be sensitively dependent on the polarization direction. As an example, we present in Figure 4a showing that CrPz-In_2Se_3 (P ↓) is metallic, with states mainly from the *d* orbital of Cr atom lifted by the polarization (Figure S5) to cross the Fermi level. However, when the polarization of the substrate is switched to the opposite direction, CrPz-In_2Se_3 (P ↑) changes into a semiconductor where the occupied *d* orbitals are located deep inside the valance band. For MnPz-In_2Se_3, the phenomena are similar, but only the down-spin channel is occupied at the Fermi level when it is placed on In_2Se_3 (P ↑), rendering the system half-metallic. Note that the metallic states are mainly contributed by the MPz molecules, and the semiconducting characteristic of In_2Se_3 is well-retained in most cases although both the valance band maximum and conduction band minimum are lifted upwards by the polarization, as shown by the DOS of In_2Se_3 at P ↑ or P ↓ polarization. Although the magnetic moment, electron transfer and adsorption energy of ScPz, NiPz and ZnPz molecules are insensitive to the polarization direction of In_2Se_3 monolayer, the corresponding electronic structures still can be affected by the ferroelectric switch. For ZnPz-In_2Se_3 (Figure 4c), the ferroelectric switch changes the band gap from 0.51 eV in ZnPz-In_2Se_3 (P ↓) to 0.84 eV in ZnPz-In_2Se_3 (P↑) due to the polarization shifted band edge states. The ferroelectric tuned electronic properties of all other MPz-In_2Se_3 systems are summarized in Figure S8. The conclusions are quite similar, indicating a high degree of

universality of the underlying mechanism for the ferroelectric tuning of electronic properties.

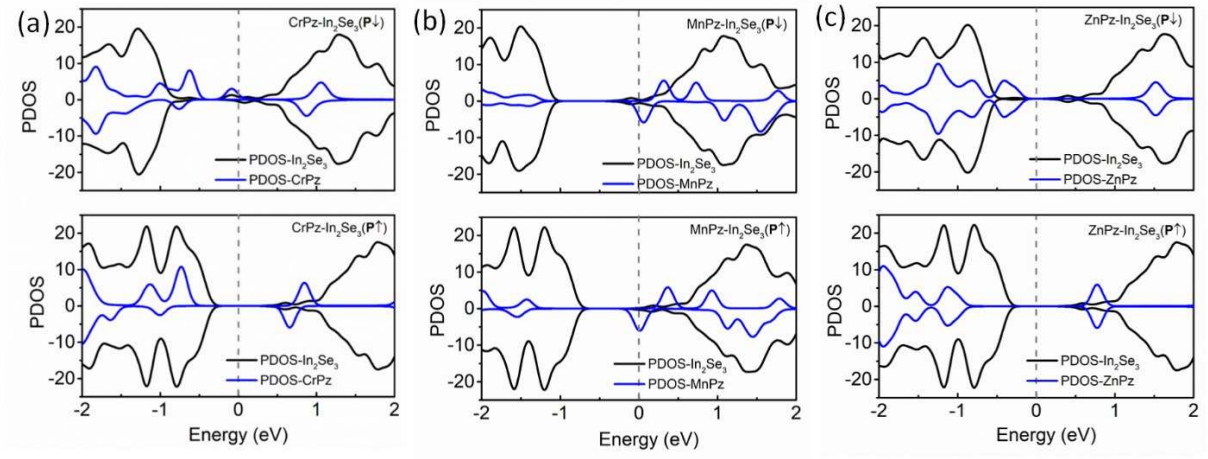

Figure 4 The spin-polarized PDOS of (a) CrPz (b) MnPz and (c) ZnPz molecule adsorbed In_2Se_3 monolayer. The Fermi level is set to zero.

Given the sensitivity of the behaviors studied in this work, it is expected that external electric fields should be able to achieve effective tuning of magnetic and electronic properties of MPz-In_2Se_3 systems. To this end, we examine CrPz-In_2Se_3 (P ↓) for its magnetic moment and electronic property variations versus electric field as shown in Figure 5a. The magnetic moment increases with the applied electric field along the +z direction, which is defined as the assigned positive direction, see Figure 1c, while the moment decreases with the electric field that is applied in the opposite (negative) direction. Interestingly, the system undergoes a metallic → half-metallic → semiconducting transition under the electric field (see Figure 5a, b). These results demonstrate the effectiveness of externally applied electric field in tuning the behaviors of MPz-In_2Se_3 systems, suggesting an added feasible avenue for tuning and controlling pertinent magnetic and electronic properties.

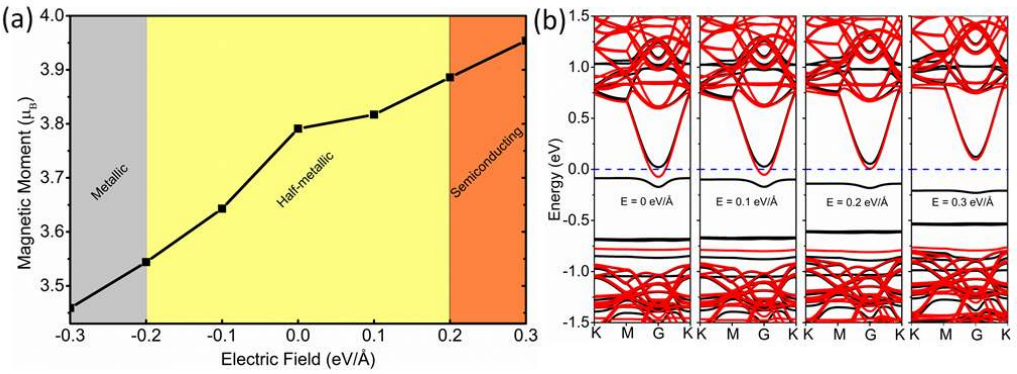

Figure 5. (a) Electric field dependence of the magnetic moment of CrPz-In_2Se_3 (P ↓). (b) Spin-polarized band structure of CrPz-In_2Se_3 (P ↓) at different electric fields. The Fermi level is set to zero. Black and red lines represent results for the spin-up and spin-down channel, respectively.

4. Conclusions

Our extensive and systematic computational studies reveal that the adsorption energy, electron transfer and magnetic moment of adsorbed MPz molecules can be effectively regulated by reversible ferroelectric polarization of In_2Se_3 monolayer. The electrostatic potential difference between the MPz molecules and In_2Se_3 monolayer with different ferroelectric polarization explains the distinct behaviors of adsorption energy and electron transfer, and the *d*-orbital occupation variation at different polarizations is responsible for the ferroelectric tuning of magnetism. Moreover, the electronic properties of the system are also modulated by the switch of ferroelectric polarization. Depending on the polarization direction, the system undergoes transitions between metallic, half-metallic and semiconducting states. The present findings hold great promise for innovative design and implementation for applications in advanced magnetic memory storage, sensor and spintronic devices.

Supporting Information

Work function of ScPz-In2Se3 (↓ and ↑); geometric structures of MPz-In_2Se_3 (M=Sc, Cr-Fe, Ni-Zn), PDOS of M (M=Sc, Ti, Cr-Zn) in the MPz adsorption system and in a free MPz molecule; magnetic moment of VPz-In_2Se_3 as a function of interlayer distance; structures of ScPz-In_2Se_3, TiPz-In_2Se_3 after movement; Spin-polarized PDOS of MPz (M=Sc, V, Fe, Co, Ni, Cu) adsorbed In_2Se_3.

Corresponding Authors

*Email: chen@physics.unlv.edu; liangzhi.kou@qut.edu.au

Notes

The authors declare no competing financial interests.

Acknowledgements

We acknowledge the grants of high-performance computer time from computing facility at the Queensland University of Technology, the Pawsey Supercomputing Centre and Australian National Facility. L.K. gratefully acknowledges financial support by the ARC Discovery Project (DP190101607).

References

(1) Žutić, I.; Fabian, J.; Sarma, S. D., Spintronics: Fundamentals and applications. *Rev. Mod. Phys.* **2004**, 76, 323.
(2) Bader, S.; Parkin, S., Spintronics. *Annu. Rev. Condens. Matter Phys.* **2010**, 1, 71-88.
(3) Wolf, S.; Awschalom, D.; Buhrman, R.; Daughton, J.; von Molnár, v. S.; Roukes, M.; Chtchelkanova, A. Y.; Treger, D., Spintronics: a spin-based electronics vision for the future. *Science* **2001**, 294, 1488-1495.
(4) Huang, X.; Dong, S., Ferroelectric control of magnetism and transport in oxide heterostructures. *Mod. Phys. Lett. B* **2014**, 28, 1430010.
(5) Nowack, K. C.; Koppens, F.; Nazarov, Y. V.; Vandersypen, L., Coherent control of a single electron spin with electric fields. *Science* **2007**, 318, 1430-1433.
(6) Rashba, E.; Efros, A. L., Efficient electron spin manipulation in a quantum well by an in-plane electric field. *Appl. Phys. Lett.* **2003**, 83, 5295-5297.
(7) George, R. E.; Edwards, J. P.; Ardavan, A., Coherent spin control by electrical manipulation of the magnetic anisotropy. *Phys. Rev. Lett.* **2013**, 110, 027601.
(8) Ohno, H.; Chiba, D.; Matsukura, F.; Omiya, T.; Abe, E.; Dietl, T.; Ohno, Y.; Ohtani, K., Electric-field control of ferromagnetism. *Nature* **2000**, 408, 944-946.
(9) Sawicki, M.; Chiba, D.; Korbecka, A.; Nishitani, Y.; Majewski, J. A.; Matsukura, F.; Dietl, T.; Ohno, H., Experimental probing of the interplay between ferromagnetism and localization in (Ga, Mn)As. *Nat. Phys.* **2010**, 6, 22-25.
(10) Vaz, C. A. F.; Hoffman, J.; Segal, Y.; Reiner, J. W.; Grober, R. D.; Zhang, Z.; Ahn, C. H.; Walker, F. J., Origin of the Magnetoelectric Coupling Effect in $Pb(Zr_{0.2}Ti_{0.8})O_3/La_{0.8}Sr_{0.2}MnO_3$ Multiferroic Heterostructures. *Phys. Rev. Lett.* **2010**, 104, 127202.
(11) Dietl, T.; Ohno, H.; Matsukura, F.; Cibert, J.; Ferrand, e. D., Zener model description of ferromagnetism in zinc-blende magnetic semiconductors. *Science* **2000**, 287, 1019-1022.
(12) Nakamura, K.; Shimabukuro, R.; Fujiwara, Y.; Akiyama, T.; Ito, T.; Freeman, A. J., Giant modification of the magnetocrystalline anisotropy in transition-metal monolayers by an external electric field. *Phys. Rev. Lett.* **2009**,

102, 187201.
(13) Nakamura, K.; Akiyama, T.; Ito, T.; Weinert, M.; Freeman, A. J., Role of an interfacial FeO layer in the electric-field-driven switching of magnetocrystalline anisotropy at the Fe/MgO interface. *Phys. Rev B* **2010**, 81, 220409.
(14) Maruyama, T.; Shiota, Y.; Nozaki, T.; Ohta, K.; Toda, N.; Mizuguchi, M.; Tulapurkar, A.; Shinjo, T.; Shiraishi, M.; Mizukami, S., Large voltage-induced magnetic anisotropy change in a few atomic layers of iron. *Nat. Nanotechnol.* **2009**, 4, 158.
(15) Taniyama, T., Electric-field control of magnetism via strain transfer across ferromagnetic/ferroelectric interfaces. *J. Phys.: Condens. Matter* 2015, 27, 504001.
(16) Eerenstein, W.; Mathur, N.; Scott, J. F., Multiferroic and magnetoelectric materials. *Nature* **2006**, 442, 759-765.
(17) Wang, J.; Neaton, J.; Zheng, H.; Nagarajan, V.; Ogale, S.; Liu, B.; Viehland, D.; Vaithyanathan, V.; Schlom, D.; Waghmare, U., Epitaxial $BiFeO_3$ multiferroic thin film heterostructures. *Science* **2003**, 299, 1719-1722.
(18) Thiele, C.; Dörr, K.; Bilani, O.; Rödel, J.; Schultz, L., Influence of strain on the magnetization and magnetoelectric effect in $La_{0.7}A_{0.3}$ MnO_3 /PMN−PT(001)(A= Sr, Ca). *Phys. Rev. B* **2007**, 75, 054408.
(19) Eerenstein, W.; Wiora, M.; Prieto, J.; Scott, J.; Mathur, N., Giant sharp and persistent converse magnetoelectric effects in multiferroic epitaxial heterostructures. *Nat. Mater.* **2007**, 6, 348-351.
(20) Wang, Z.; Zhang, T.; Ding, M.; Dong, B.; Li, Y.; Chen, M.; Li, X.; Huang, J.; Wang, H.; Zhao, X., Electric-field control of magnetism in a few-layered van der Waals ferromagnetic semiconductor. *Nat. Nanotechnol.* **2018**, 13, 554-559.
(21) Yan, Y.; Zhou, X.; Li, F.; Cui, B.; Wang, Y.; Wang, G.; Pan, F.; Song, C., Electrical control of Co/Ni magnetism adjacent to gate oxides with low oxygen ion mobility. *Appl. Phys. Lett.* **2015**, 107, 122407.
(22) Zhao, Y.; Zhang, J. J.; Yuan, S.; Chen, Z., Nonvolatile electrical control and heterointerface-induced half-metallicity of 2D ferromagnets. *Adv. Funct. Mater.* **2019**, 29, 1901420.
(23) Lu, Y.; Fei, R.; Lu, X.; Zhu, L.; Wang, L.; Yang, L., Artificial Multiferroics and Enhanced Magnetoelectric Effect in van der Waals Heterostructures. *ACS Appl. Mater. & Interfaces* **2020**, 12, 6243-6249.
(24) Gong, C.; Kim, E. M.; Wang, Y.; Lee, G.; Zhang, X., Multiferroicity in atomic van der Waals heterostructures. *Nat. Commun.* **2019**, 10, 1-6.
(25) Cui, C.; Hu, W.-J.; Yan, X.; Addiego, C.; Gao, W.; Wang, Y.; Wang, Z.; Li, L.; Cheng, Y.; Li, P., Intercorrelated in-plane and out-of-plane ferroelectricity in ultrathin two-dimensional layered semiconductor In_2Se_3. *Nano Lett.* **2018,** 18, 1253-1258.
(26) Zhou, Y.; Wu, D.; Zhu, Y.; Cho, Y.; He, Q.; Yang, X.; Herrera, K.; Chu, Z.; Han, Y.; Downer, M. C., Out-of-plane piezoelectricity and ferroelectricity in layered α-In_2Se_3 nanoflakes. *Nano Lett.* **2017**, 17, 5508-5513.
(27) Liao, M.-S.; Watts, J. D.; Huang, M.-J., FeII in different macrocycles: Electronic structures and properties. *The J. Phys. Chem. A* **2005**, 109, 7988-8000.
(28) Sun, Y.; Chen, K.; Jia, L.; Li, H., Toward understanding macrocycle specificity of iron on the dioxygen-binding ability: a theoretical study. *Phys. Chem. Chem. Phys.* **2011**, 13, 13800-13808.
(29) Shen, J.; Wang, M.; Gao, J.; Han, H.; Liu, H.; Sun, L., Improvement of Electrochemical Water Oxidation by Fine-Tuning the Structure of Tetradentate N4 Ligands of Molecular Copper Catalysts. *ChemSusChem* **2017**, 10, 4581-4588.
(30) Yang, Q.; Zhong, T.; Tu, Z.; Zhu, L.; Wu, M.; Zeng, X. C., Design of Single-Molecule Multiferroics for Efficient Ultrahigh-Density Nonvolatile Memories. *Adv. Sci.* **2019**, 6, 1801572.
(31) Kresse, G.; Furthmüller, J., Efficiency of ab-initio total energy calculations for metals and semiconductors using a plane-wave basis set. *Computat. Mater. Sci.* **1996**, 6, 15-50.
(32) Blöchl, P. E., Projector augmented-wave method. *Phys. Rev. B* **1994**, 50, 17953.
(33) Kresse, G.; Joubert, D., From ultrasoft pseudopotentials to the projector augmented-wave method. *Phys. Rev. B* **1999**, 59, 1758.
(34) Perdew, J. P.; Burke, K.; Ernzerhof, M., Generalized gradient approximation made simple. *Phys. Rev. Lett.* **1996**, 77, 3865.
(35) Anisimov, V. I.; Aryasetiawan, F.; Lichtenstein, A., First-principles calculations of the electronic structure and spectra of strongly correlated systems: the LDA+ U method. *J. Phys.: Condens. Matter* **1997**, 9, 767.
(36) Zhou, J.; Sun, Q., Magnetism of phthalocyanine-based organometallic single porous sheet. *J. Am. Chem. Soc.* **2011**, 133, 15113-15119.
(37) Panchmatia, P. M.; Sanyal, B.; Oppeneer, P. M., GGA+ U modeling of structural, electronic, and magnetic

properties of iron porphyrin-type molecules. *Chem. Phys.* **2008**, 343, 47-60.
(38) Grimme, S., Semiempirical GGA- type density functional constructed with a long- range dispersion correction. *J. Comput. Chem.* **2006**, 27, 1787-1799.
(39) Aguirre, M.; Cárdenas-Jirón, G.; Toro-Labbé, A.; Zagal, J., A theoretical procedure to determine interaction energies in complex systems: application to the oxygen–iron tetraazaporphyrin interaction. *J. Mol. Struct.: THEOCHEM* **1999**, 493, 219-224.
(40) Wang, F.; Cao, B.; To, W.-P.; Tse, C.-W.; Li, K.; Chang, X.-Y.; Zang, C.; Chan, S. L.-F.; Che, C.-M., The effects of chelating N 4 ligand coordination on Co (ii)-catalysed photochemical conversion of CO_2 to CO: reaction mechanism and DFT calculations. *Catal. Sci. & Technol.* **2016**, 6, 7408-7420.
(41) Ding, W.; Zhu, J.; Wang, Z.; Gao, Y.; Xiao, D.; Gu, Y.; Zhang, Z.; Zhu, W., Prediction of intrinsic two-dimensional ferroelectrics in In_2Se_3 and other III_2-VI_3 van der Waals materials. *Nat. Commun.* **2017**, 8, 1-8.
(42) Peng, R.; Ma, Y.; Zhang, S.; Huang, B.; Kou, L.; Dai, Y., Self-doped p–n junctions in two-dimensional In_2X_3 van der Waals materials. *Mater. Horiz.,* **2020**, 7, 504-510.
(43) Fu, C.-F.; Sun, J.; Luo, Q.; Li, X.; Hu, W.; Yang, J., Intrinsic electric fields in two-dimensional materials boost the solar-to-hydrogen efficiency for photocatalytic water splitting. *Nano Lett.* **2018**, 18, 6312-6317.
(44) Osamura, K.; Murakami, Y.; Tomiie, Y., Crystal Structures of α-and β-indium selenide, In_2Se_3. *J. Phys. Soc. Jpn.* **1966**, 21, 1848-1848.
(45) Cho, W. J.; Cho, Y.; Min, S. K.; Kim, W. Y.; Kim, K. S., Chromium porphyrin arrays as spintronic devices. *J. Am. Chem. Soc.* **2011**, 133, 9364-9369.
(46) Liao, M.-S.; Scheiner, S., Electronic structure and bonding in metal porphyrins, metal= Fe, Co, Ni, Cu, Zn. *J. Chem. Phys.* **2002**, 117, 205-219.
(47) Henkelman, G.; Arnaldsson, A.; Jónsson, H., A fast and robust algorithm for Bader decomposition of charge density. *Comput. Mater. Sci.* **2006**, 36, 354-360.

Table of Contents